Fabrication Uncertainty and Noise Issues in High-Precision MEMS Actuators and Sensors

Young-Ho Cho, Won Chul Lee, and Ki-Ho Han

Abstract— **We present technical issues involved in the development of actuators and sensors for applications to high-precision Micro Electro Mechanical System (MEMS). The technical issues include fabrication uncertainty and noise disturbance, causing major difficulties for MEMS to achieve high-precision actuation and detection functions. For nano-precision actuators, we solve the fabrication instability and electrical noise problems using digital actuators coupled with nonlinear mechanical modulators. For the high-precision capacitive sensors, we present a branched finger electrodes using high-amplitude anti-phase sensing signals. We also demonstrate the potential applications of the nanoactuators and nanodetectors to high-precision positioning MEMS.**

Index Terms—**MEMS, Actuators, Sensors, Fabrication uncertainty, Noise instability, High-precision MEMS, Digital actuation, Nonlinear modulation, Branched-finger electrodes, high-amplitude signals**

I. Introduction

Recent advances in MEMS technology make it possible to fabricate mechanical, optical and biofluidic components in extremely small sizes. Performance of optical, biological and inertial MEMS, however, is governed not only by the sizes but also by the precision of the actuation and detection devices. High-precision manipulation of photons and biological nanosubstances is required for optical and biological MEMS. High-precision detection of microstructural motion is demanded for nano-positioning and inertial MEMS. Major technical difficulties in the high-precision MEMS are arising from the fabrication uncertainty and electrical noise problems. In this paper, we present high-precision actuators and detectors, overcoming the technical limitations placed by the conventional MEMS technology.

II. Nanoactuators

Recently, mechanical modulation [1,2] of a digital actuation has been suggested for high-precision positioning applications due to the nature of the mechanical modulators immune to electrical noise. Ultimate precision of the mechanical modulators [1,2], however, are constrained by the precision of the digital actuation. Displacement stroke of the digital actuators contains an inherent uncertainty in the order of $\pm 0.1\mu m$, generated by the micromachining error and/or the sidewall roughness of mechanical stoppers. In this work, we propose NMDA having a built-in nonlinear mechanical modulator for reducing the displacement error of the digital microactuator, thereby producing a purified high-precision motion stroke, required for nano-precision positioning devices. The function and concept of the nonlinear mechanical modulator are equivalent to those of the nonlinear electrical switch, such as a Zener diode.

We present the concept of a nonlinearly modulated

Manuscript received November 15, 2002; revised December 12, 2002.
Digital Nanolocomotion Center
Korea Advanced Institute of Science and Technology 373-1 Guseong-dong, Yuseong-gu, Daejeon 305-701, Republic of Korea
E-mail : dnc@kaist.ac.kr **Tel** : +82-42-869-8691
Fax : +82-42-869-8690

digital actuator (NMDA) and the experimental verification of its capability for producing a high-precision digital stroke. The NMDA (Fig.1), composed of a digital microactuator and a nonlinear micro-mechanical modulator, that modulates or purifies the motion(x_{in}) of the digital actuator using the nonlinear motion limiting function of the modulator.

Figure 2 illustrates a simple model of the micromechanical modulator, composed of a pair of the micromechanical spring-mass set. Figure 3 illustrates the modulation curves of the linear and nonlinear modulators.

The linear modulator(Fig.2) having two linear springs may reduce the magnitude of errors (Fig.3a), but it cannot reduce the error-to-displacement ratio (i.e., the noise-to-signal ratio). On the other hand, the nonlinear modulator (Fig.2), composed of a nonlinear spring (k_2) and a linear spring (k_1), reduces the magnitude of errors as well as the relative error using the slope change of the nonlinear modulation curve (Fig.3b). We have designed two kinds of prototypes (Fig.4, Table 1) using the folded beams and the fixed-fixed beams as the linear and nonlinear springs, respectively. From finite element analysis, we designed the displacement modulation curves (Fig.5) of the linear and nonlinear modulators, having an identical input and output pair of 15.2μm and 5.4μm. In the portion A of Fig.5b, we find that NMDA also maintains stable displacement output against the over-etching and under-etching of the micromechanical

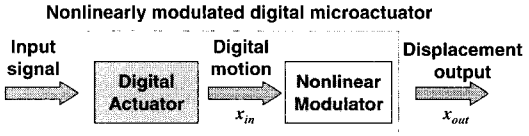

Fig. 1. Configuration of the nonlinearly modulated digital actuator (NMDA)

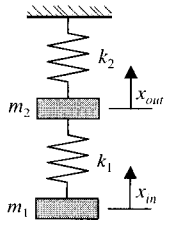

Fig. 2. Model of the micromechanical modulator, composed of two springs, k1 and k2.

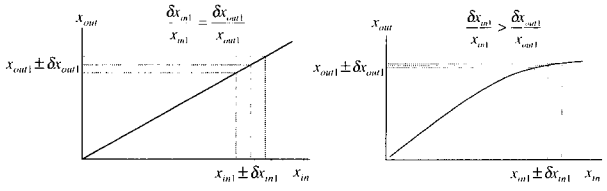

Fig. 3. Displacement modulation curves of the micromechanical modulators: (a) linear modulator; (b) nonlinear modulator.

Table 1. Measured dimensions of the fabricated devices.

Structure thickness		t	40 μm
Beam width		w	2.4 μm
Length of beam 1		L_1	500 μm
Length of beam 2	Linear modulator	$(L_2)_L$	416 μm
	Nonlinear modulator	$(L_2)_{NL}$	500 μm
Digital input displacement		x_{in1}	15.2 μm
Proof mass 1		m_1	13.5 μg
Proof mass 2		m_2	2.53 μg
Stiffness of spring 1		k_1	1.11 N/m
Stiffness of spring 2	Linear modulator	$(k_2)_L$	1.93 N/m
	Nonlinear modulator	$(k_2)_{NL}$	1.11~4.1N/m

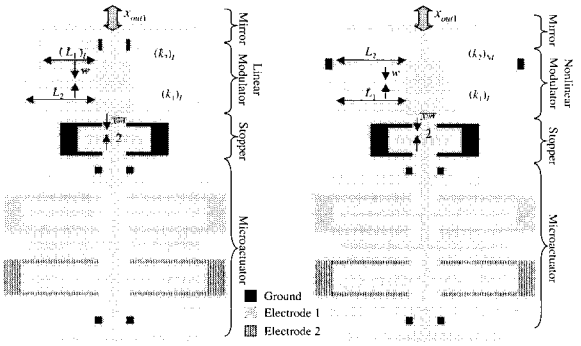

Fig. 4. Schematic view of the mechanically modulated digital microactuators using two different modulators: (a) linear modulator; (b) nonlinear modulator.

beam springs. Figure 6 shows the one-mask fabrication process for two different prototypes shown in Figs. 7 and 8.

For a nano-precision measurement, we use the modified Mach-Zehnder interferometer shown in Fig.9a, where the laser beam has been focused on the

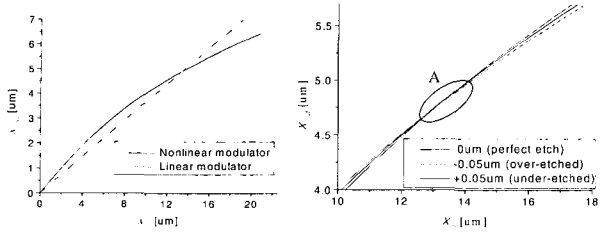

(a) (b)

Fig. 5. Displacement modulation curves of the linear and nonlinear micromechanical modulators: (a) overall curves; (b) Nonlinear modulation curves depending on the microfabrication error of ±0.05μm

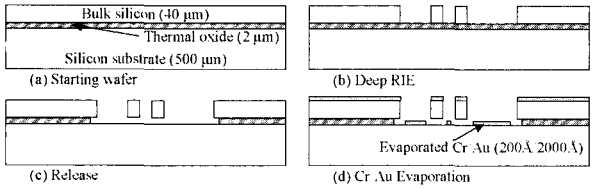

Fig. 6. Microfabrication process of the mechanically modulated microactuators.

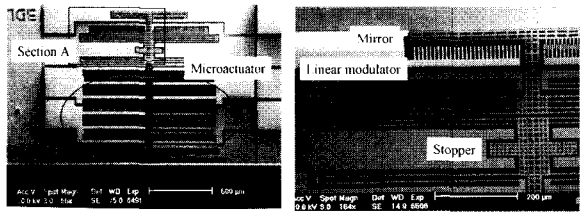

(a) (b)

Fig. 7. SEM photographs of the linearly modulated microactuator: (a) overall structure ; (b) an enlarged view of the Section A in (a).

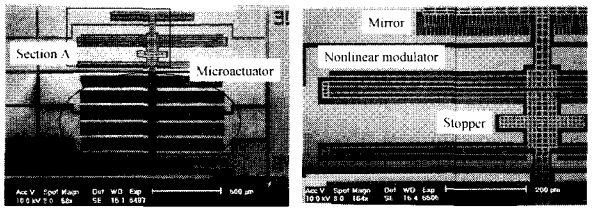

(a) (b)

Fig. 8. SEM photographs of the nonlinearly modulated microactuator: (a) overall structure ; (b) an enlarged view of the Section A in (a).

Table 2. Experimental and theoretical values of the repeatability in the modulated displacement output of the linearly and nonlinearly modulated digital microactuators.

Prototype	Experimental	Theoretical
LMDA	27.8±2.9 nm	25.8 nm
NMDA	12.3±2.9 nm	15.4 nm

Table 3. Experimental and theoretical values of the repeatability in the linearly modulated output of the LMDA and NMDA.

Prototype	Experimental	Theoretical
LMDA	17.7±7.7 nm	15.1 nm
NMDA	12.3±7.2 nm	9.2 nm

micromirror (Fig.9b) attached to the modulated output port. For the digital actuation of 60Hz, the modulated displacement (x_{out}) has been measured from the distance between two stable portions (A and B in Fig.10a). The measurement uncertainty of 2.9nm has been due to the jitter of the signals, as shown in Fig.10b. Figure 11 compares the measured and estimated modulation curves of the fabricated micromechanical modulators for varying displacement input. For the precision evaluation, we perform repeated output measurements (7 times) from the linearly and nonlinearly modulated digital microactuators, both producing the output in the range of 5.46±0.10μm. Experimental values of the repeatability in Table 2 have been defined as the double of the standard deviation in the repeated measurement. Table 2 demonstrates that NMDA shows the repeatability of 12.3±2.9nm, superior to that of 27.8±2.9nm achieved by the linearly modulated digital microactuators (LMDA).

Additionally, we have designed and fabricated another set of prototypes, where an identical linear modulator has been attached to the output port of the previous prototypes (Figs.7 and 8). From the repeated measurements (Table 3) of the modulated output, we also find that the linearly modulated output of the NMDA shows better repeatability than that of LMDA, confirming the NMDA can be served as a digital input purifier for micromechanical modulator systems.

III. NANODETECTORS

We present high-resolution capacitive nanodetectors and their applications to microaccelerometers, whose low-noise force-balancing effect has been achieved by using branched finger electrodes with high-amplitude anti-phase sense voltage. The present microaccelrometer reduces the total noise to 5.5μg/$\sqrt{Hz}$, while the Conven-

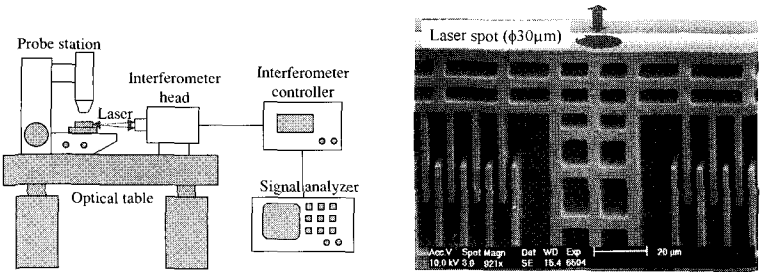

(a) (b)

Fig. 9. Modulated displacement output measurement: (a) experimental apparatus; (b) laser spot on the vertical mirror.

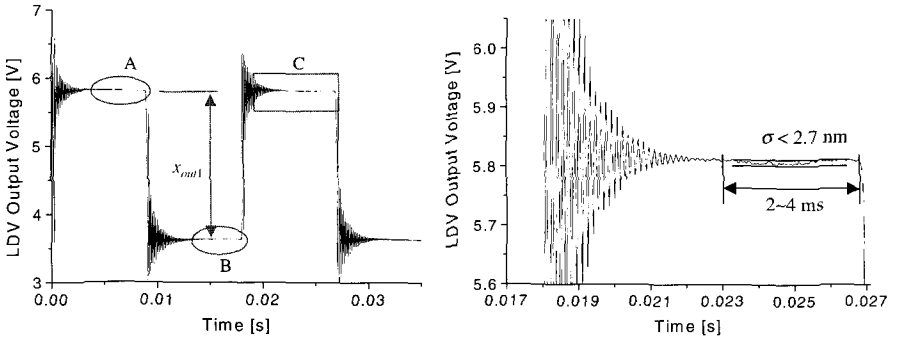

(a) (b)

Fig. 10. Modulated displacement output measurement: (a) displacement output signal; (b) an enlarged view of the portion C in (a).

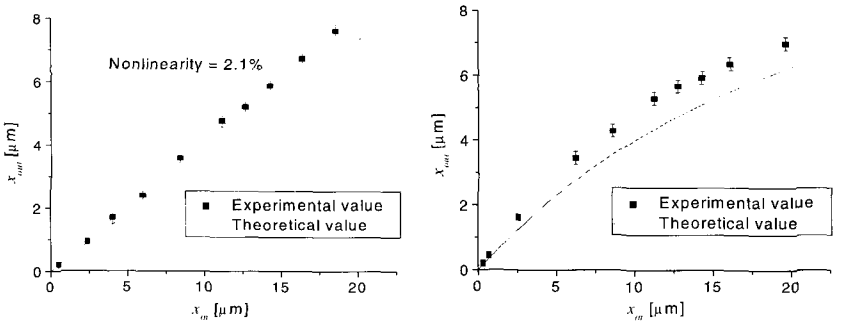

(a) (b)

Fig. 11. Displacement modulation curves of the linear and nonlinear micromechanical modulators: (a) linear modulator; (b) nonlinear modulator.

tional devices have shown the noise level of 25~800μg/$\sqrt{Hz}$ [3~8]. First, we reduce the mechanical noise of the nanodetector to the level of 5.5μg/$\sqrt{Hz}$ by increasing the proof-mass based on deep RIE process of an SOI wafer. Then, we reduce the electrical noise as low as 0.6μg/$\sqrt{Hz}$ using an anti-phase sense voltage of 250kHz 19V obtained from a DC-to-DC voltage multiplier. The nonlinearity problem arising in the high-voltage capacitive detection has been solved by a new electrode design of branched finger form. Combined use of the new electrode design and the high-amplitude anti-phase sense voltage has generated self force-balancing effects, resulting in a good linearity of 0.044% with an 140% increase of the bandwidth from 726Hz to 1,734Hz.

In the conventional capacitive detectors of surface-micromachined accelerometers [3,4], the total noise has been governed mainly by mechanical noise. Recent studies have focused on the reduction of the mechanical noise by increasing the proof-mass and have used the methods of multi wafer bonding [5], combined surface- and bulk-micromachining [6], or RIE of SOI wafers [7],

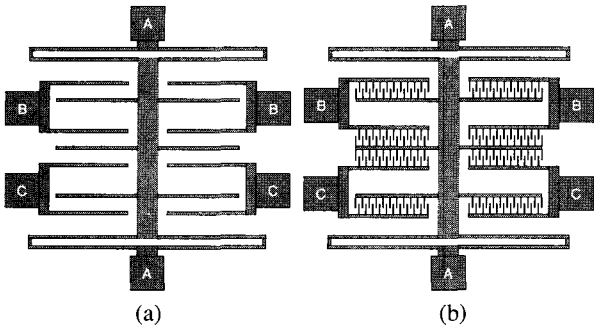

Fig. 12. Comparison of the electrodes of capacitive micro-accelerometers: (a) conventional straight finger electrodes; (b) present branched finger electrodes.

Table 4. Measured dimension of the microaccelerometer.

Structure thickness (t)	40 [μm]
Suspension width (w)	3.7 [μm]
Suspension length (l)	580 [μm]
Finger gap (x)	1.8 [μm]
Finger pitch (p)	9 [μm]
Suspension stiffness (k)	1.06 [N/m]
Proof-mass (m)	51 [μg]
Total initial capacitance (C_1=C_2)	2.4 [pF]
Overall size	2.0×2.2 [mm×mm]

* Based on the E=130 [GPa]

thereby making the mechanical noise lower than the electrical noise. Nowadays, the electrical noise of microaccelerometers places major technical barrier to achieve a high-resolution. In this paper, we propose a new microaccelerometer design for a low electrical noise, high resolution performance.

In the conventional straight finger electrodes (Fig.12a) [8], the high-amplitude sense voltage causes nonlinearity and instability problems. Thus, we have devised a new type of electrodes having branched fingers (Fig.12b), thereby introducing self-balancing effects for the enhanced linearity and stability of the high-voltage capacitive detection. Figure 13 illustrates single-mask RIE process for the microaccelerometers described in Table 4 and Fig.14. Figure 15 shows the readout technique for the microaccelerometers using the 250kHz anti-phase high-voltage copping method. The motion of the movable electrode of Fig.15 generates an electrostatic force opposing the motion, providing more simple and automated force-balancing scheme compared to the conventional force-balancing scheme [9] requiring additional negative electromechanical feedback loop. Figures 16a and 16b show the output signal and its power spectrum measured from the fabricated microaccelerometer for a 10Hz, 1g sinusoidal acceleration at the sense voltage, *Vs*, of 19V, respectively.

The signal-to-noise ratio of 105dB (Fig.16b) demonstrates the detection resolution of $5.5\mu g/\sqrt{Hz}$. Other peaks observed at harmonic frequencies in Fig.5b are the noises generated by the electromagnetic exciter.

Figure 17 compares the measured and estimated noise components of the fabricated microaccelerometer for varying sense voltage. In Fig.17a, the total noise of $5.5\mu g/\sqrt{Hz}$ has been measured at *Vs*=19V, resulting in

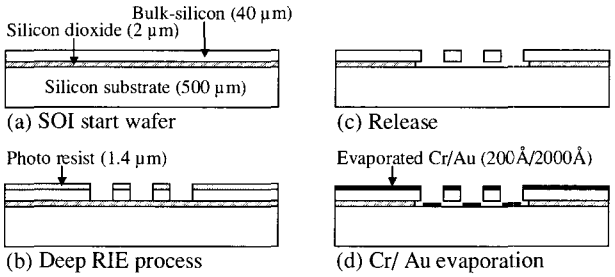

Fig. 13. Single-mask fabrication process.

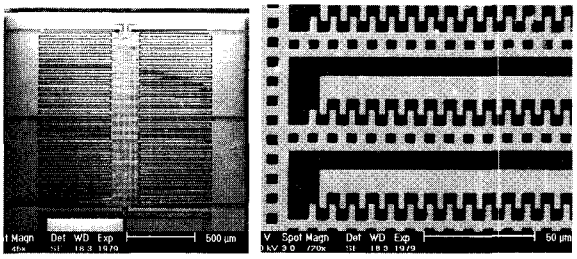

Fig. 14. Fabricated microaccelerometer: (a) top view; (b) enlarged view of the branched finger electrodes.

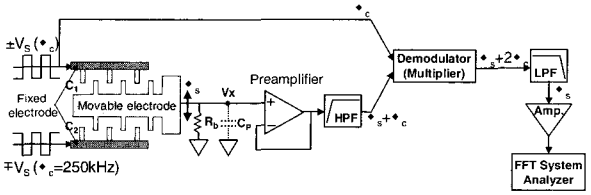

Fig. 15. Schematic of the readout technique for the micro-accelerometer on an electromagnetic exciter.

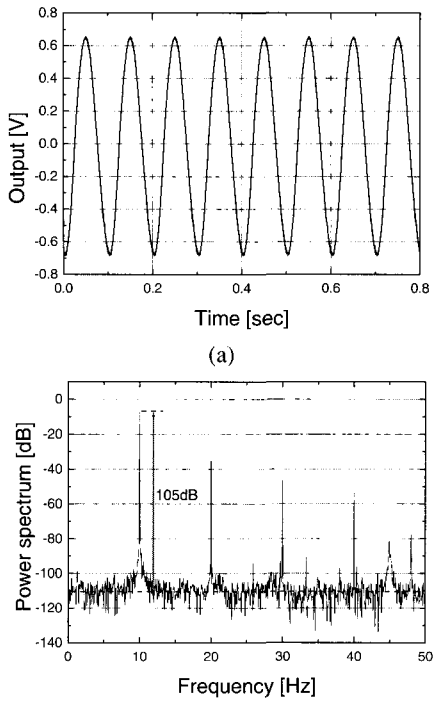

Fig. 16. Output of the fabricated microaccelerometer measured at the sense voltage of 19V for a 10Hz, 1g sinusoidal acceleration: (a) output signal; (b) power spectrum.

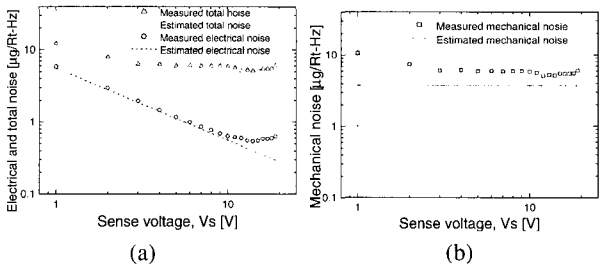

Fig. 17. Measured and estimated noise levels of the microaccelerometer for varying sense voltage, Vs: (a) electrical and total noise; (b) mechanical noise.

Table 5. Performance of the microaccelerometer at the sense voltage of 19V.

Detection range	± 2 [g]
Resonant frequency	1.73 [kHz]
Resolution	5.5 [μg/$\sqrt{\text{Hz}}$]
Sensitivity	0.638 [V/g]
Linearity	0.044 [%]
Minimum detectable proof-mass displacement	0.019 [nm]

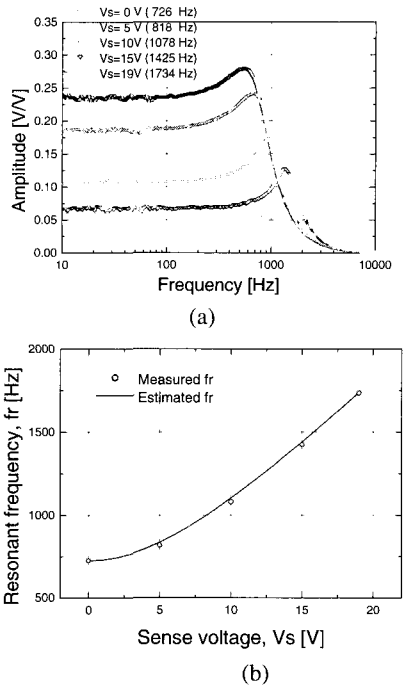

Fig. 18. Frequency response of the microaccelerometer for varying sense voltage, Vs: (a) amplitude response; (b) resonant frequency response.

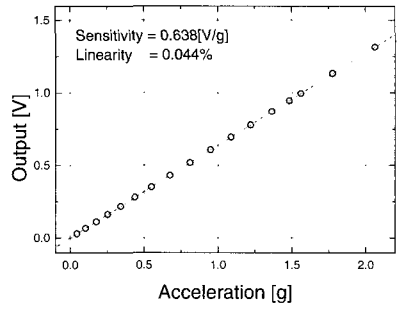

Fig. 19. Microaccelerometer output for varying acceleration measured for 10Hz acceleration at the sense voltage of 19V.

a 220% noise reduction compared to that of order of magnitude improvement compared to the electrical noise of 6μg/$\sqrt{\text{Hz}}$ at Vs=1V. For the sense voltage higher than 1V (Fig.17a and 17b), the electrical noise of the microaccelerometer becomes smaller than the constant mechanical noise level of 5.5μg/ $\sqrt{\text{Hz}}$. Figure 18 illustrates the self force-balancing effect of the branched finger electrodes for varying sense voltage. The electrostatic stiffness caused by the electrostatic balancing force has been increased to 6.09N/m at Vs=19V from that of 1.06N/m at Vs=0V, thus producing additional stiffness at the rate of 0.014N/m/V^2 for the

enhanced linearity and bandwidth of the micro-accelerometer at the higher sense voltage. Figure 19 shows the measured sensitivity and linearity of 0.638V/g and 0.044%, respectively. Other measured performance of the microaccelerometer has been summarized in Table 5.

IV. Summary and Conclusions

We identified and discussed the fabrication uncertainty and noise disturbance issues constraining the performance and precision of MEMS. We presented feasible methods to solve the technical issues for improving the precision of MEMS sensors and actuators.

First, we presented the nonlinearly modulated digital actuator (NMDA) and the experimental verification of its capability for producing a high-precision digital stroke. We designed and fabricated the conventional linear and proposed nonlinear modulators, connected to the digital microactuators, which had an identical input and output pair of 15.2μm and 5.4μm. From the experimental study, the measured linear and nonlinear modulation curves coincided well with the theoretically estimated curves. In precision evaluation using the measured repeatability, the NMDA showed the repeatability of 12.3±2.9nm, superior to that of 27.8±2.9nm achieved by the LMDA. We experimentally verified the capability of NMDA for producing a high-precision digital stroke, showing potential for nano-precision positioning applications.

Second, we presented a high-resolution capacitive detector and its applications to microaccelerometers using the branched finger electrodes with the high-amplitude sense voltage. We reduced the mechanical noise to the level of $5.5\mu g/\sqrt{Hz}$ by increasing the proof-mass based on deep RIE process of an SOI wafer, and the electrical noise as low as $0.6\mu g/\sqrt{Hz}$ by using the high-amplitude sense voltage of 19V. In order to improve the nonlinearity caused from the high-amplitude sense voltage, we modified the conventional straight finger electrode into the branched finger electrode. We obtained the self force-balancing effect, which produce stiffness increase rate of $0.014N/m/V^2$ for enhanced linearity and bandwidth of the microaccelerometer. We also measured the sensitivity and linearity of 0.638V/g and 0.044%, respectively. Consequently, by the branched finger electrode with the high-amplitude sense voltage, we could be maintains proper bandwidth by induction of the self force-balancing effect, though the heavy proof-mass is used for reducing the mechanical noise, and also obtained good linearity.

Acknowledgement

This work has been supported by the National Creative Research Initiative Program of the Ministry of Science and Technology (MOST) under the project title of "Realization of Bio-Analogic Digital Nanoactuators."

References

[1] H. Toshiyoshi, D. Kobayashi, M. Mita, G. Hashiguchi, H. Fujita, J. Endo and Y. Wada, "Micro Electro Mechanical Digital-to-Analog Converter," *Transducers '99*, pp. 994-997.

[2] R. Yeh, R.A. Conant and K.S. Pister, "Mechanical Digital-to Analog Converters," *Transducers '99*, pp. 998-1001.

[3] K.H.-L. Chau, S.R. Lewis, Y. Zhao, R.T. Howe, S.F. Bart, and R.G. Marcheselli, "An Integrated Force-balanced Capacitive Accelerometer for Low-g Applications," *Transducers'95*, 1995, pp. 593-596.

[4] E. Boser, R.T. Howe, "Surface Micromachined Accelerometers," *IEEE J. Solid-State Circuit*, Vol.31, No. 3, 1996, pp. 366-375.

[5] K. Warren, "Navigation Grade Silicon Accelerometer with Sacrificially Etched SIMOX and BESOI Structure," *Tech. Dig. Solid-State Sensors and Actuators Workshop*, Hilton Head Island, SC, June 1994, pp. 69-72.

[6] N. Yazdi, A. Salian, K. Najafi, "A High Sensitivity Capacitive Microaccelerometer with a Folded-electrode Structure," *MEMS'99*, pp. 600-605.

[7] M.A. Lemkin. T.N. Juneau, W.A. Clark, T.A. Roessig and T.J. Broshihan, "A Low-noise Digital Accelerometer using Integrated SOI-MEMS Technology," *Transducers'99*, pp. 1294-1297.

[8] M. Offenberg, etal., *Society of Automotive Engineers*, SP-1133, 1996, pp. 35-41.

[9] W. Kuehnel, S. Sherman, "A Surface Micromachined Silicon Accelerometer with On-chip Detection Circuitry," *Sensor and Actuators*, A 45, 1994, pp. 7-16.

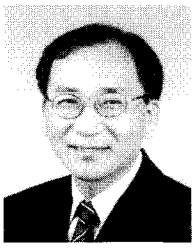

Young-Ho Cho received the B.S. degree *summa cum laude* from Yeungnam University, Daegu, Korea, in 1980; the M.S. degree from the Korea Advanced Institute of Science and Technology (KAIST), Seoul, Korea, in 1982; and the Ph.D. degree from the University of California at Berkeley for his electrostatic actuator and crab-leg microflexure research completed in December, 1990.

From 1982 to 1986 he was a Research Scientist of CAD/CAM Research Laboratory, Korea Institute of Science and Technology (KIST), Seoul, Korea. During 1987-1991, he worked as a Post-Graduate Researcher (1987-1990) and a Post-Doctoral Research Associate (1991) of the Berkeley Sensor and Actuator Center (BSAC) at the University of California at Berkeley. In August 1991, Dr. Cho moved to KAIST, where he is currently an Associate Professor in the Departments of BioSystems & Mechanical Engineering as well as the Director of Digital Nanolocomotion Center.

Dr. Cho's research interests are focused on the optomechanical and biofluidic microsystems with micro/nano-scaled actuators and detectors for photon manipulation and biomedia processing. In Korea, he has served as the Chair of MEMS Division in Korean Society of Mechanical Engineers, the Chair of Steering Committee in Korea National MEMS Programs, the Chair of Steering Committee in Korean Next Generation Technology Development Program, the Leader of Nanobio-Group in National NanoForum and the Committee of National Nanotechnology Planning Board. Dr. Cho has also served for international technical society as the General Co-Chair of IEEE MEMS Conference 2003, the Program Committee of IEEE Optical MEMS Conference, the Chief Delegate of the Republic of Korea in World Micromachine Summit. Dr. Cho is a member of IEEE and ASME.

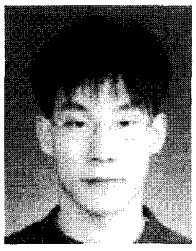

Won Chul Lee was born in Seoul, Korea, in 1978. He received the B.S. degree in 1999 and the M.S. degree from mechanical engineering at Korea Advanced Institute of Science and Technology (KAIST), Daejeon, Korea, for his nonlinearly modulated digital microactuators in 2001.

He is currently a Ph.D. student in BioSystems department at KAIST. His research interests include high-precision microactuators and microdetectors for optical and biomedical applications.

Ki-Ho Han was born in Busan, Korea, in 1970. He received the B.S. degree in 1993 and the M.S. degree in 1996 from electrical engineering at Korea Advanced Institute of Science and Technology (KAIST), Daejeon, Korea, and the Ph.D. degree from mechanical engineering at KAIST for his high-resolution capacitive subnanometric motion detectors using branched finger electrodes with high-amplitude sense voltage in 2002.

He is currently working as a Postdoctoral Associate in the Micro Instrumentation Research laboratory at the Georgia Institute of Technology, GA. His research interests include BioMEMS transducers, inertial microdevices, small signal detection circuitry and ASIC development for fully-integrated microdevices and microsystems.